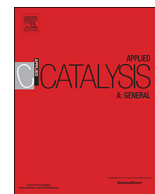




ELSEVIER

Contents lists available at ScienceDirect

Applied Catalysis A, General

journal homepage: www.elsevier.com/locate/apcata

The main factors affecting the catalytic properties of Ru/Cs-HPA systems in one-pot hydrolysis-hydrogenation of cellulose to sorbitol

Nikolay V. Gromov^{a,b,*}, Tatiana B. Medvedeva^a, Oxana P. Taran^{a,c,d}, Maria N. Timofeeva^{a,b}, Olivier Said-Aizpuru^e, Valentina N. Panchenko^{a,b}, Evgeniy Yu. Gerasimov^a, Ivan V. Kozhevnikov^f, Valentin N. Parmon^a

^a Borekov Institute of Catalysis SB RAS, 630090, Lavrentiev Av., 5, Novosibirsk, Russia

^b Novosibirsk State Technical University, 630092, Karl Marx Av., 20, Novosibirsk, Russia

^c Institute of Chemistry and Chemical Technology SB RAS, FRC Krasnoyarsk Science Center SB RAS, 660036, Akademgorodok 50/24, Krasnoyarsk, Russia

^d Siberian Federal University, 660041, Svobodny Av., 79, Krasnoyarsk, Russia

^e Ecole Normale Supérieure de Lyon, 69007, Allée d'Italie 46, Lyon, France

^f Department of Chemistry, University of Liverpool, Liverpool, L69 7ZD, United Kingdom

ARTICLE INFO

Keywords:

Hydrolysis

-hydrogenation

Cellulose

Sorbitol

Ruthenium

Cesium salt of heteropoly acid

ABSTRACT

One-pot conversion of mechanically activated cellulose to sorbitol was investigated over bifunctional catalysts based on Ru (0.6, 1 and 3 wt.%) and cesium salts of heteropoly acids (HPA) Cs_{2.1}H_{0.9}PW₁₂O₄₀ and Cs₃HSiW₁₂O₄₀ (Cs-PW and Cs-SiW, respectively). The maximal yield of sorbitol equal to 59 % and selectivity 94 % were achieved over the 1%Ru/Cs₃HSiW₁₂O₄₀ catalyst. Physicochemical and catalytic data showed that the rate-determining step, i.e. the hydrolysis of cellulose, depended on the surface acidity of catalysts, whereas Ru content in catalyst affected both the hydrolysis and the hydrogenation steps. The kinetic parameters for one-pot conversion of cellulose were determined by mathematical modeling approach and were successfully used for the prediction of the yields of sorbitol and mannitol.

1. Introduction

In the past decade, intense research activities have been focused on the search for alternative resources for energy and chemistry. The renewable and carbon-neutral plant raw materials are among the most promising resources [1–3]. The ever increasing attention is paid to the conversion of one of the main components of the plant raw materials – cellulose (a glucose homopolymer, up to 70 %) [4,5] – to valuable chemicals and liquid fuels [3,6].

The catalytic transformation of cellulose under mild conditions unfortunately is a complex task due to the robust crystalline structure of cellulose. Traditional technologies for cellulose processing include the step of cellulose hydrolysis over soluble mineral acid catalysts (H₂SO₄, HCl etc.) to produce glucose, which may be transformed into platform molecules and fuels in subsequent steps. Such the valuable chemicals as sorbitol and mannitol can be produced from glucose over catalysts containing Ni, Ru, [7,8]. These products are widely used in the chemical and food industries, pharmaceuticals, medicine etc. [1].

The main drawbacks of traditional technologies for cellulose processing are corrosive activity of soluble acid catalysts at high reaction

temperatures and the formation of dangerous waste waters. These problems can be solved by designing new catalytic systems for the cellulose processing. Here, of special note is the development of one-pot transformation of cellulose to desirable products with the use of bifunctional catalysts. This one-pot processing appears very promising due to elimination of technological stages of intermediates isolation and purification which gives economic and environmental advantages.

Nowadays, there are two strategies for conducting one-pot hydrolysis-hydrogenation of cellulose into polyols (Scheme 1). The first approach suggested by Balandin et al. [9] is the use of liquid acid (as catalyst for hydrolysis) in combination with a supported metal material (as the hydrogenation catalyst) in one reactor. This way allows polyols, namely, sorbitol, mannitol etc. to be synthesized (Table S1, Supporting Information (SI)) [10–12].

The rate and selectivity of the process is effected significantly both the chemical nature of the metal and the acid type. Thus, Ni, Pt, Ir, Rh, Pd, or Ru fixed on different supports can be used [13–15]. It should be emphasized that yields of hexitols (sorbitol and mannitol) are higher over Ru-containing catalysts compared to non-ruthenium ones. Also for cellulose to be transformed efficiently over catalysts without

* Corresponding author.

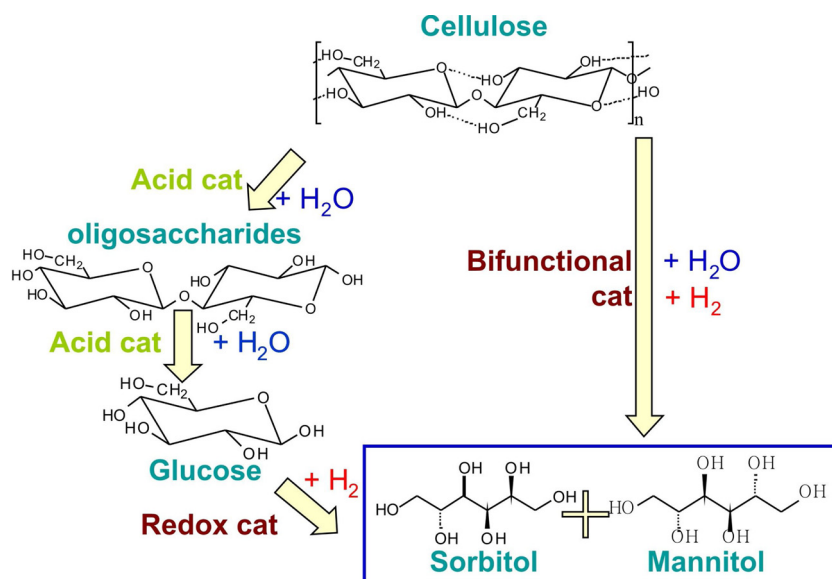
E-mail address: gromov@catalysis.ru (N.V. Gromov).

<https://doi.org/10.1016/j.apcata.2020.117489>

Received 12 December 2019; Received in revised form 10 February 2020; Accepted 28 February 2020

Available online 28 February 2020

0926-860X/ © 2020 Elsevier B.V. All rights reserved.



Scheme 1. Possible approaches to transformation of cellulose to sorbitol.

ruthenium, severe conditions (463–518 K and 5–6 MPa) have to be used whereas as the reaction can be conducted under milder conditions (423–458 K, 5 MPa) over Ru-based systems [16,17]. Thus, one can conclude that Ru-based catalysts seem to be most promising.

HCl and H₂SO₄ can be used as catalysts for hydrolysis of cellulose to glucose (Scheme 1). The yields of hexitols reach 33–37 % over a combination of soluble acids and Ru-containing catalysts. Apart from mineral acids (HCl and H₂SO₄), heteropoly acids (HPA) also were applied in this process [12,18]. For example, in the presence of "H₄SiW₁₂O₄₀ - Ru/C" system the conversion of ball-milled cellulose reached 99 % and the total yield of target products (sorbitol and mannitol) was ca. 85 % [12]. Note, that the application of H₄SiW₁₂O₄₀ instead of mineral sulfuric acid under identical conditions increased significantly the efficiency of cellulose conversion (82 % vs 56 %) and selectivity to hexitols (49 % vs 28 %) (Table S1, SI). The high solubility of HPA can be overcome through the use of their insoluble cesium salts (Cs-HPA) that facilitates significantly the catalyst recovery procedure [19]. Geboers et al. [19] showed that Cs_{3.5}H_{0.5}SiW₁₂O₄₀ and Cs_{2.5}H_{0.5}PW₁₂O₄₀ in combination with Ru/C gave total yield of hexitols of 55 and 45 %, respectively. It should be emphasized that the mixture of two solid catalysts is more effective than the 'soluble HPA - Ru/C' system for processing ball-milled microcrystalline cellulose, when the highest yields of hexitols reached no more than 18 and 41 % in the presence of H₄SiW₁₂O₄₀ and H₃PW₁₂O₄₀, respectively, under identical conditions [20]. Hence, Cs-HPAs were more active than their fully protonated counterparts, probably, due to their high surface acidity and hydrophobicity. The same total yields of the polyalcohols were reached three times faster over Cs_{2.5}H_{0.5}PW₁₂O₄₀ - Ru/C under identical reaction conditions and at identical calculated concentrations of H⁺.

The second approach to the one-pot hydrolysis-hydrogenation of cellulose into polyols is based on the application of a bifunctional catalyst. One of the advantages of bifunctional catalysts is the selectivity increasing due to acceleration of mass transfer of the intermediates between acid and metal active centers. Different type porous supports (carbon, mesoporous silica materials, zeolites etc.) were suggested for preparing such bifunctional catalysts (Table S1, SI) [21,22]. Presumably, severe experimental conditions, i.e. high temperature (483–503 K) and/or longer reaction time (24–36 h), must be used to achieve the high conversion of insoluble cellulose. For example, the maximal total yield of sorbitol and mannitol equal to 27 % was reached over 4.0 wt% Ru/SBA-15 [23], and 22–31 % over 2.5 wt. % Ru/HUSY under severe conditions [24]. The use of Ru/Cs-HPA systems made it

possible to carry out the process under mild conditions [25]. Thus, *one-pot* hydrolysis-hydrogenation of ball-milled cellulose into sorbitol with 40 % yield proceeds at 433 K and 2 MPa of H₂ over 1%Ru/Cs₃PW₁₂O₄₀ [25].

Since the *one-pot* hydrolysis-hydrogenation of cellulose in one-pot operation proceeds through consecutive/tandem reactions (depolymerization, hydrolysis and hydrogenation) over bifunctional catalyst, thus productivity and selectivity of the overall process depends on the ratio of reaction rates, which is affected by the number and properties of each the catalytic sites. Studies of cellulose hydrolysis over acid cesium salts Cs_xH_{3-x}PW₁₂O₄₀ (x = 1–3) [26] showed that the glucose yield depends on the number of acid sites which were determined by the concentration of cesium ions. Highly negatively charged heteropolyacids H₅BW₁₂O₄₀ and H₅AlW₁₂O₄₀ with stronger Brønsted acidity were more active to hydrolysis of cellulose [27]. On the other hand, Shimizu et al. [28] studied the conversion of cellulose or cellobiose in the aqueous media and showed that the yield of glucose correlated with the deprotonation enthalpy of soluble HPAs and mineral acids. These data lead us to suppose that the number of acid sites in the bifunctional Ru/Cs-HPA catalysts also should influence the yields of the main products such as sorbitol and mannitol.

Moreover, we can assume that the reaction rate and the product yields depend on the size of ruthenium nanoparticles because the hydrogenation process depends strongly on the size of metal particles on the support surface [29–31]. Hydrogenation of arabinose and galactose into arabinitol and galactitol over supported Ru/C catalysts with the cluster size ranging from 1 to 8 nm was found to be structure sensitivity [32]. The chemical state of Ru species also influences on the conversion of cellulose to sorbitol. Generally, Ru⁰ nanoparticles are believed to be the active phase for hydrogenation [10]. Kobayashi et al. [33] suggested that cationic Ru species were the active phase over a Ru/C catalyst which catalysed hydrogenation of cellulose with 2-propanol as the source of hydrogen.

We report here the progress of our research aimed at the design of Ru/Cs-HPA systems for one-pot hydrolysis-hydrogenation of cellulose into polyols. The purpose of the study was to evaluate the main factors affecting the catalytic properties of Ru/Cs-HPA systems. The attention was mainly focused on the effects of surface acidity and aggregation state of Ru nanoparticles. Analysis of the main factors that affect the reaction rate and the isomer selectivity was based on a combination of catalytic, kinetic and physicochemical methods. We also provided kinetic analysis of experimental data using mathematical

model.

2. Experimental

2.1. Materials

5-Hydroxymethylfurfural (> 98 %, Acros), D-fructose (> 99 %, Sigma-Aldrich), D-mannose (> 99 %, Sigma-Aldrich), D-glucose (99 %, Fisher Chemical), D-cellobiose (> 99 %, Alfa Aesar), mannitol (> 98 %, Alfa Aesar), sorbitol (98 %, Alfa Aesar) were used as HPLC standards.

Catalysts were prepared using $\text{H}_3\text{PW}_{12}\text{O}_{40}\cdot 19\text{H}_2\text{O}$, $\text{H}_4\text{SiW}_{12}\text{O}_{40}\cdot 7.5\text{H}_2\text{O}$, Cs_2CO_3 (99.5 %, Acros Organic), $\text{Ru}(\text{NO})(\text{NO}_3)_3$ (31.5 % Ru content, Alfa Aesar) and carbon material Sibunit-4 (Center of New Chemical Technologies of the FRC Boreskov Institute of Catalysis SB RAS, Omsk, Russia). Microcrystalline cellulose (> 99 %, fraction < 0.10 mm, Vekton Co., Russia) was used as a substrate. Argon (99.998 %) as an inert gas and hydrogen (99.99 %) was used for hydrogenation. Water purified with a Milli-Q unit (Millipore, France) was used for preparation of all catalysts and solutions.

2.2. Mechanical activation of cellulose

Microcrystalline cellulose was activated in a discrete action planetary mill Pulverizette 5 (Fristch, Germany) with a 0.25 dm³ bowl, seven balls (20 mm diameter), cellulose sample weight 15 g, working power 1.5 kW, centrifugal acceleration ($g = 9.81 \text{ m s}^{-2}$) 22 g. Activation time was 40 min.

The size of activated cellulose particles was determined using an optical microscope Biomed-5 (LLC Biomed-M, Russia) equipped with a digital camera (Fig. S1, SI).

XRD analysis of the microcrystalline and mechanically activated cellulose was conducted using a Bruker D8 diffractometer (Germany) with Cu radiation ($\lambda = 1.5418 \text{ \AA}$) in 0.05° steps at 2 θ range from 10 to 40° (Fig. S1-S2, SI). The degree of cellulose crystallinity was calculated as the ratio of summed area of peaks of crystalline cellulose to the summed area of all peaks [34].

2.3. Synthesis of catalysts

$\text{Cs}_{2.1}\text{H}_{0.9}\text{PW}_{12}\text{O}_{40}$ and $\text{Cs}_3\text{HSiW}_{12}\text{O}_{40}$ were synthesized from HPAs ($\text{H}_3\text{PW}_{12}\text{O}_{40}$ and $\text{H}_4\text{SiW}_{12}\text{O}_{40}$) and Cs_2CO_3 according to the procedure described in literature [35]. Chemical composition of cesium salts is shown in Table S2 (SI). The main physicochemical characteristics of Cs-HPA are shown in Figs. S3-S6 (SI).

Bifunctional catalysts of $\text{Ru}/\text{Cs}_{2.1}\text{H}_{0.9}\text{PW}_{12}\text{O}_{40}$ and $\text{Ru}/\text{Cs}_3\text{HSiW}_{12}\text{O}_{40}$ were prepared by the incipient wetness impregnation of the supports by aqueous $\text{Ru}(\text{NO})(\text{NO}_3)_3$ solution. The load of Ru was 0.6, 1 and 3 wt.%. The amount of water corresponding to the wettable pore network of the support and containing the appropriate amount of metal was dispersed on the support [36]. The HPA salts impregnated by ruthenium precursor were reduced in flowing hydrogen at 573 K (heating rate 1 °C min⁻¹ from room temperature to 573 K) for 2 h. A similar procedure was used for supporting Ru on Sibunit-4 [37]. The main physicochemical characteristics of Ru/Cs -HPA are shown in Figs. S3-S6 (SI).

2.4. Instrumental measurements

Texture of the prepared samples was characterized by low-temperature nitrogen adsorption at 69 K using an ASAP-2400 apparatus (Micromeritics, USA). All the samples were vacuumized at 403–423 K. Specific surface areas were calculated using the BET model and STSA equation, as well as the comparative method with the Cabor BP 280 carbon as the reference. Pore size distribution was estimated based on QSDFT and NLDFT calculations.

A JEM-2010 instrument (JEOL, Japan) with the accelerating voltage 200 kV and resolution 1.4 Å was used for transmission electron microscopic (TEM) studies. For the studies, catalytic particles were mounted on perforated carbon substrates fixed on copper nets.

X-ray diffraction patterns were acquired using a X-ray diffractometer (ThermoARL) with Cu-K α ($\lambda = 1.5418 \text{ \AA}$) radiation. The POLYCRYSTAL program package was used to determine the unit lattice constants by the least squares method [38].

Chemical analyses were done by an inductively coupled plasma-atomic emission spectrometry (ICP-AES) using a PERKIN-ELMER instrument OPTIMA 4300.

Brønsted and Lewis surface acidity was analyzed by IR-spectroscopy using pyridine as the probe molecule (SI) [39]. IR spectra were acquired on a Shimadzu FTIR-8300S spectrometer in the range between 400 and 6000 cm⁻¹ with a resolution of 4 cm⁻¹.

DR UV-VIS studies of the Ru/Cs -HPA samples were performed with a Shimadzu UV-2501PC spectrophotometer with a DR attachment ISR-240A.

2.5. Catalyst tests

Hydrolysis-hydrogenation of cellulose was conducted in a high-pressure autoclave (Autoclave Engineers, USA) at 453 K and 5 MPa of hydrogen under vigorous stirring 1500 rpm. Contents of cellulose and catalyst were both 10 g L⁻¹. Weighed cellulose and catalyst samples were placed to the reactor, after that 45 mL of water were added. The reactor was closed and cleaned with argon, and fed with hydrogen (5 MPa), then heating was started. As soon as the required temperature was reached (that took ca. 20 min), a zero sample was collected using a sampler. Samples to be analyzed were drawn from the autoclave during the reaction in 0, 1, 2, 3, 5 and 7 h. Sample volume was 1 mL.

Reaction products were analyzed by HPLC (Shimadzu Prominence LC-20) equipped with refractive index and diode array detectors and Rezex RPM-Monosaccharide Pb²⁺ column thermostated at 343 K. Deionized water prepared in a Milli-Q apparatus (Millipore, France) was used as the eluent at the rate of 0.6 mL min⁻¹.

The total organic carbon (TOC) content was determined in the solution after the reaction using a Multi N/C 2100S TOC Analyzer (Analytik Jena, Germany). A 500 μL aliquot of the reaction mixture was added into an analyzer injector. The amount of organic carbon (g L⁻¹) was calculated based on the calibrations.

Each cellulose depolymerization experiment was repeated three times. Each analysis of the reaction mixtures was carried out three times. The standard deviation of the results was less 2%.

The yields of the reaction products were calculated according to the formula [40,41]:

$$Y = \frac{n \cdot C_{\text{product}} \cdot V}{6 \cdot (m_{\text{cell}} / M_{\text{glucan}})} \cdot 100\%$$

where Y is the yield, C_{product} (mol L⁻¹) is the product concentration, V is the reaction volume (0.045 L), n is the coefficient equal to the content of carbon atoms in a product molecule, m_{cell} is mass of cellulose charged into the autoclave (0.45 g), M_{glucan} is the molar mass of glucan unit (162 g mol⁻¹).

The selectivity of products was calculated as follows:

$$S = \frac{\omega \cdot C_{\text{product}}}{C_{\text{TOC}}} \times 100\%$$

where S is the selectivity, ω is the coefficient equal to the content of carbon atoms in a product molecule, C_{product} is the product concentration, C_{TOC} is the total concentration of organic carbon detected with TOC analyzer.

3. Results and discussion

3.1. Mechanical activation of cellulose

Pre-activation of crystalline cellulose is well known to make possible shortening the reaction time of catalytic hydrolysis-hydrogenation and to reduce the process temperature [42]. Therefore, the initial crystalline cellulose underwent mechanical activation to reduce the crystallinity degree and to destroy the structure of the cellulose. The morphology and particle sizes of cellulose are shown in Fig. S1A (SI). One can see the pristine cellulose consists of the aggregates of rod-shaped crystals of $114 \pm 35 \mu\text{m}$ in length. Mechanical activation of cellulose in the planetary-type mill during 40 min changes strongly its morphology and particle sizes (Fig. S1B, SI). According to XRD data (Fig. S2, SI), the crystallinity degree of pristine cellulose is 92 %, whereas the crystallinity of the activated sample equals to 36 %.

3.2. Synthesis and investigation of Ru/Cs-HPA samples

Ru/Cs-HPA samples were prepared by incipient wetness impregnation of Cs-PW and Cs-SiW using the aqueous Ru-salt solution. Chemical compositions of Cs-PW and Cs-SiW are shown in Table S2 (SI). According to Kobayashi et al. [15], the nature of precursor affects the catalytic behavior of Ru-based catalysts. Thus, the total yield of sorbitol and mannitol was 37.9 and 57.4 % over $\text{Ru}_{\text{Cl}}/\text{Al}_2\text{O}_3$ and $\text{Ru}_{\text{N}}/\text{Al}_2\text{O}_3$ prepared from RuCl_3 and $\text{RuNO}(\text{NO}_3)_3$, respectively. In view of the results reported elsewhere [15], we used $\text{RuNO}(\text{NO}_3)_3$ as the precursor [15]. First of all, IR spectroscopy was used for monitoring the stability of the Keggin structure heteropoly anion impregnated with Ru ($\text{NO}(\text{NO}_3)_3$) and then reduced in the H_2 atmosphere at 573 K. The bands at 1080 cm^{-1} ($\nu_{\text{as}}(\text{P-O}_a)$), 981 cm^{-1} ($\nu_{\text{as}}(\text{W-O}_d)$), 891 cm^{-1} ($\nu_{\text{as}}(\text{W-O}_b\text{-W})$) and 799 cm^{-1} ($\nu_{\text{as}}(\text{W-O}_c\text{-W})$) were observed in the IR spectrum of Cs-PW and bands at 981 cm^{-1} ($\nu_{\text{as}}(\text{W-O}_d)$), 930 cm^{-1} ($\nu_{\text{as}}(\text{Si-O}_a)$), 879 cm^{-1} ($\nu_{\text{as}}(\text{W-O}_b\text{-W})$) and 798 and 793 cm^{-1} ($\nu_{\text{as}}(\text{W-O}_c\text{-W})$) were observed in the spectrum of Cs-SiW (Fig. S3 (SI)). These bands are intrinsic to heteropoly anions with the Keggin structure $[\text{PW}_{12}\text{O}_{40}]^{3-}$ and $[\text{SiW}_{12}\text{O}_{40}]^{4-}$ [35,43]. The procedure of Ru supporting gave rise to appearance of a band at 923 cm^{-1} in the IR spectra of Ru/Cs-PW and Ru/Cs-SiW. Moreover, the band at 793 cm^{-1} ($\nu_{\text{as}}(\text{W-O}_c\text{-W})$) in the spectrum of Ru/Cs-SiW shifted to 798 cm^{-1} that pointed to the interaction between Ru and corner oxygen atoms in the WO_6 octahedrons. In addition, new bands at 893 cm^{-1} in the spectra of Ru/Cs-HPA may indicate the formation of $\text{W-O}\rightarrow\text{Ru}$ bonds [44].

Data of DR–UV/vis spectroscopy also point to the interaction between Ru nanoparticles and heteropoly anion. One can be seen from DR–UV/vis spectra of Ru/Cs-PW and Ru/Cs-SiW (Fig. S4 (SI)), an intense absorption peak at 280 nm assigned to a charge transfer bond within the Keggin units ($\text{O}^{2-} \rightarrow \text{W}^{6+}$) was observed in the spectra of Cs-HPA salts. Supporting Ru on Cs-PW caused the appearance of a broad band at 300–500 nm assigned to Ru^{3+} ions [44]. This band decreased in intensity with an increase in the Ru content. At the same time, another absorption band appeared at 400–800 nm, its intensity also depended on the content of supported ruthenium. The dependence of the band intensities on the proportion of supported ruthenium may indicate a change in the size of Ru particles. A similar dependence of band intensity at 300–500 nm on the size of Ru particles also was demonstrated in studying the $\text{Ru}/\text{Al}_2\text{O}_3$ system under the action of microwave irradiation [44].

The size of ruthenium particles on the surface of Cs-HPA was estimated using TEM. There are ruthenium nanoparticles on the micrographs (Fig. 1) with rather narrow particle size distribution (0.9–1.4 nm) (Table 1). An increase in the Ru content in Cs-PW and Cs-SiW resulted in changes in the particle size from 0.9 to 1.0 nm for the Ru/Cs-PW catalysts and from 0.9 to 1.4 nm for the Ru/Cs-SiW samples (Table 1, Fig. 1). The conclusion on the small size of the ruthenium nanoparticles was also supported by the XRD data. Reflections of

ruthenium particles were not observed in the diffraction patterns of Ru/Cs-PW and Ru/Cs-SiW samples (Fig. S5, SI).

Textural properties of the bifunctional catalysts were studied using low-temperature adsorption-desorption of nitrogen. Isotherms of adsorption-desorption of nitrogen on Cs-HPA and Ru/Cs-HPA and textural data are shown in Fig. S6 (SI) and Table 1, respectively. Cs-HPA salts possess high specific surface area equal to 159 and $195 \text{ m}^2 \text{ g}^{-1}$ for Cs-PW and Cs-SiW, respectively. The Cs-HPAs contain micropores and some mesopores. The data obtained demonstrated that both the specific surface area and micropore volume decreased upon supporting ruthenium on the cesium salt of HPA (Table 1). S_{BET} comes to $140 \text{ m}^2 \text{ g}^{-1}$ for Cs-PW and $110 \text{ m}^2 \text{ g}^{-1}$ for Cs-SiW.

3.3. Catalytic properties of Cs-salts

Catalytic properties of Cs-HPA salts in hydrolysis of cellulose were tested first. The reaction was carried out at 5 MPa H_2 and 453 K. The main results are shown in Fig. S7 (SI) and Table 2. Glucose was the main product over Cs-salts (Table 2, runs 1 and 6). The formation of cellobiose, mannose, fructose, 5-hydroxymethylfurfural, furfural, levulinic and formic acids also was revealed. The total yield of the products in 1 and 2 h of the reaction is higher in the presence of Cs-SiW (35 and 39 %) than over Cs-PW (29 and 22 %) (Fig. S7, SI). The selectivity of Cs-PW is lower than that Cs-SiW. In 7 h, the glucose yields were 4 and 14 % (selectivity 22 and 50 %) over Cs-PW and Cs-SiW, respectively. This difference can be explained by the difference in nature of the acid sites. IR spectroscopic studies with pyridine as the probe molecule revealed that there are 263 and $101 \mu\text{mol g}^{-1}$ of Brønsted acid sites (BAS) and 20 and $23 \mu\text{mol g}^{-1}$ of Lewis acid sites (LAS) on the surface of Cs-PW and Cs-SiW, respectively (Table S3, SI). The higher Brønsted acidity of Cs-PW resulted in lower selectivity to glucose in comparison with that of Cs-SiW (Table 2, runs 1 and 6).

3.4. Catalytic properties of Ru-containing bifunctional systems based on Cs-HPA salts

The reaction rate, selectivity and product distribution changed considerably after supporting Ru on Cs-HPA (Table 2). The hydrolysis-hydrogenation took place over Ru/Cs-PW and Ru/Cs-SiW catalysts, and the hydrogenation of glucose produced mainly sorbitol at a high selectivity (94–96 %). The main side product was mannitol at the yield not higher than 4%. The maximal yield of sorbitol up to 63 % at 94 % selectivity was observed over 1%Ru/Cs-SiW in 5 h of the reaction (Fig. 2). However, the yield of sorbitol decreased slightly to 59 % in 7 h (Table 2, run 10). Note that maximal yield over the other catalysts were reached in 7 h. For example, 1% Ru/Cs-PW produced 49 % of sorbitol (Table 2, run 3).

This is better than the results reported in literature [25]: hydrolysis-hydrogenation of ball-milled cellulose over similar catalyst (1%Ru/ $\text{Cs}_3\text{PW}_{12}\text{O}_{40}$) gave 40 % of sorbitol at 433 K in 24 h. To our knowledge, Ru/Cs-SiW was used in cellulose hydrolysis-hydrogenation for the first time in this work. Some authors reported that the presence of catalysts containing Ru or Ni nanoparticles and W structures may produce of ethylene glycol and propylene glycol from polysaccharides [47–49]. High yields of ethylene glycol was observed over tungsten carbides supported on activated carbons [48,49]. However we did not detect ethylene glycol and propylene glycol among the reaction products.

It is interesting to compare activity of Ru/Cs-PW and Ru/Cs-SiW in 3 h of the reaction. According to experimental data (Table 2), the yield of sorbitol increased in the following series:

$$3\% \text{Ru/Cs-PW} < 3\% \text{Ru/Cs-SiW} < 0.6 \quad \% \text{Ru/Cs-SiW} < 1\% \text{Ru/Cs-PW} < 1\% \text{Ru/Cs-SiW}$$

There may be two reasons for the difference in catalytic properties of Ru/Cs-SiW and Ru/Cs-PW. First, inspection of the experimental data leads to conclude that the yield of sorbitol depends on the content of ruthenium in Ru/Cs-HPA system. The yield of sorbitol is higher over

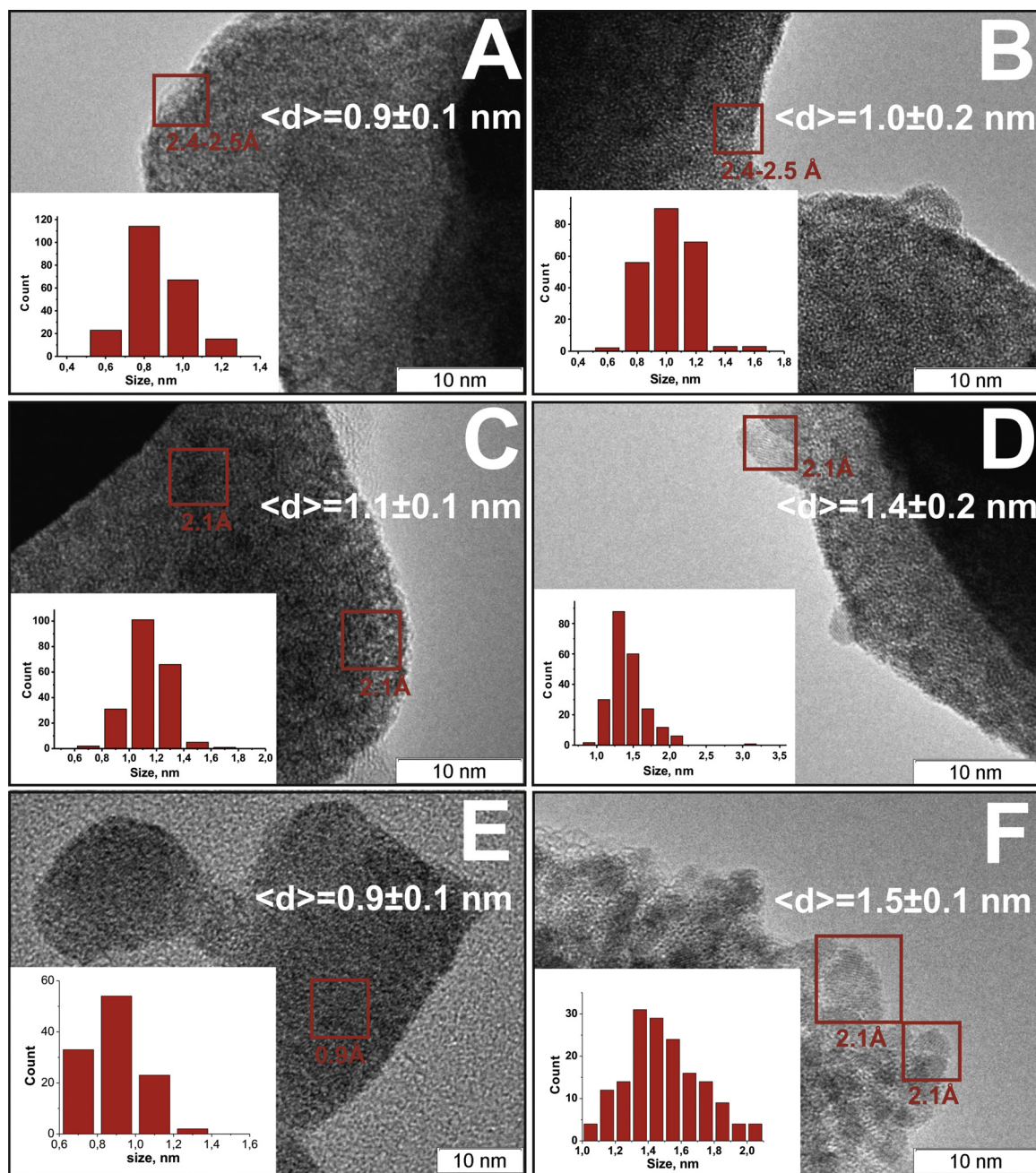


Fig. 1. TEM micrographs and Ru particle size distribution of 1% Ru/Cs-PW (A), 3%Ru/Cs-PW (B), 1%Ru/Cs-SiW (C), 3%Ru/Cs-SiW (D), 0.6 %Ru/Cs-SiW (E), and 1%Ru/Cs-SiW after the reaction (F).

Table 1

Textural properties of Cs-HPA and Ru/Cs-HPA systems.

Catalyst	Textural properties [a]				Ru particle size (nm)
	S_{BET} (m^2g^{-1})	S_{meso} (m^2g^{-1})	$V_{\Sigma n}$ (cm^3g^{-1})	V_{μ} (cm^3g^{-1})	
$\text{Cs}_{2.1}\text{H}_{0.9}\text{PW}_{12}\text{O}_{40}$	159	31	0.092	0.064	–
1%Ru/Cs-PW	140	17	0.078	0.045	0.9 ± 0.1
3%Ru/Cs-PW	140	21	0.074	0.035	1.0 ± 0.2
$\text{Cs}_3\text{HSiW}_{12}\text{O}_{40}$	195	9	0.094	0.074	–
0.6 %Ru/Cs-SiW	110	10	0.092	0.050	0.9 ± 0.1
1%Ru/Cs-SiW	110	11	0.091	0.041	1.1 ± 0.2
3%Ru/Cs-SiW	110	10	0.074	0.025	1.4 ± 0.2

[a] S_{BET} – Specific surface area; S_{meso} – Mesopore surface area; V_{Σ} – Total pore volume; V_{μ} – Micropore volume.

Table 2
Catalytic properties of Cs-HPA and Ru/Cs-HPA systems in hydrolysis-hydrogenation of cellulose [a].

N	Catalyst	Time (h)	Sorbitol		Mannitol		Glucose		5-HMF		$\Sigma_{\text{yield}}^{[b]}$ (%)
			S (%)	Y (%)	S (%)	Y (%)	S (%)	Y (%)	S (%)	Y (%)	
1	Cs _{2.1} H _{0.9} PW ₁₂ O ₄₀	7 ^[c]	0	0	0	0	22	4	11	3	18
2	1%Ru/Cs-PW	3	97	38	3	1	0	0	0	0	39
3		7	94	49	6	3	0	0	0	0	52
4	3%Ru/Cs-PW	3	94	31	6	2	0	0	0	0	33
5		7	94	44	4	2	2	1	0	0	47
6	Cs ₃ HSiW ₁₂ O ₄₀	7 ^[c]	0	0	0	0	50	14	17	4	28
7	0.6 %Ru/Cs-SiW	3	84	37	7	3	9	4	0	0	44
8		7	87	49	7	4	6	3	0	0	56
9	1%Ru/Cs-SiW	3	95	58	5	3	0	0	0	0	61
10		7	94	59	6	4	0	0	0	0	63
11	3%Ru/Cs-SiW	3	96	33	4	1	0	0	0	0	34
12		7	94	36	6	2	0	0	0	0	38
13	3%Ru/C + Cs-SiW	3	86	13	14	2	0	0	0	0	15
14		7	90	8	10	1	0	0	0	0	9
15	3%Ru/C	3 ^[c]	9	1	38	4	6	1	40	4	10
16		7	17	1	50	3	0	0	33	2	6
17	1%Ru/Cs ₃ PW ₁₂ O ₄₀	5 ^[d]	n.d.	43	n.d.	2.1	n.d.	0.3	n.d.	n.d.	n.d.
18	Cs _{2.5} H _{0.5} PW ₁₂ O ₄₀ -5 wt% Ru/C	13 ^[e]	n.d.	58 ^[f]	n.d.	n.d.	n.d.	n.d.	n.d.	n.d.	n.d.
19	Cs _{3.5} H _{0.5} SiW ₁₂ O ₄₀ -5 wt% Ru/C	8 ^[e]	n.d.	59 ^[f]	n.d.	n.d.	n.d.	n.d.	n.d.	n.d.	n.d.
20	3.2%Ru/16.7 %PW ₁₂ /MIL-100(Cr)	10 ^[g]	n.d.	57.9	n.d.	6.6	n.d.	0	n.d.	n.d.	n.d.

[a] Experimental conditions: 450 mg of cellulose, 450 mg of catalyst, 45 ml of water, 453 K, 5 MPa of H₂. [b] The total yield based on the cellulose loaded. [c] Fructose was determined by HPLC. [d] 100 mg of catalyst, 100 mg of cellulose, 15 ml of water, H₂, 2 MPa of H₂, 433 K, 24 h reaction time. The catalyst was pretreated in H₂ at 573 K for 5 h [25]. [e] 1 g of CsHPA about 0.5 g ([H⁺] = 1.5 mM), 250 mg of Ru/C, 50 ml of water, 5 MPa of H₂, 443 K [19]. [f] Total yield of hexytols (sorbitol + mannitol). [g] 50 mg of cellulose, 30 mg of Ru-PTA/MIL-100(Cr) (3.2 wt.%Ru, 16.7 wt.% PTA), 8 ml of water, 463 K, 2 MPa of H₂. [45].

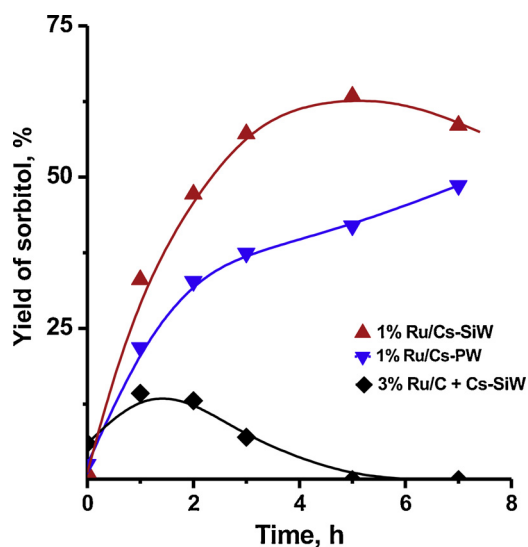


Fig. 2. Kinetics curves of sorbitol accumulation during hydrolysis-hydrogenation of mechanically activated cellulose. (Experimental conditions: 10 g L⁻¹ of cellulose, 10 g L⁻¹ of catalyst, 5 MPa of H₂, 453 K).

catalysts bearing 1% of Ru. For example, the sorbitol yield is almost doubled over 1%Ru/Cs-SiW compared to the yield over 3%Ru/Cs-SiW. 0.6 %Ru/Cs-SiW demonstrates lower activity than 1%Ru/Cs-SiW. Notice, however, that Ru/Cs-SiW is more active than Ru/Cs-PW at identical metal contents in spite of the higher dispersion of Ru in the latter. We can assume that this phenomenon is related to the difference in metal states on the surface of Cs-HPA. TEM studies of Ru nanoparticles supported on Cs-SiW (Fig. 1) revealed that the Ru-Ru interatomic distance equals mainly 2.1 Å that is typical for metal state of Ru [44], while the distance equal to 2.4 Å also is observed that may be an evidence of the existence of RuO_x particles. At the same time, the average interatomic distance in Ru/Cs-PW sample is close to RuO_x particles and equals 2.4–2.5 Å.

Another reason for the difference in catalytic properties of Ru/Cs-

SiW and Ru/Cs-PW systems may be the different nature and number of acid sites (Table S3, SI). In general, the yield of sorbitol decreases with decreasing number of BAS and increasing number of LAS. This trend can indicate that cellulose hydrolysis is the limiting stage in the hydrolysis-hydrogenation. Moreover, the observed higher activity of 1% Ru/Cs-HPA in comparison with that of 3%Ru/Cs-HPA is related to the difference of the number of BAS and the change of LAS nature. The catalysts contain two types of LAS, namely LAS formed by ruthenium and tungsten (LAS_{Ru} and LAS_{HPA}). There are other facts to support that contradiction. The point of intersection of two correlations between the Ru loading and the number of LAS and BAS in Ru/Cs-SiW is observed at 1 wt% of Ru (Fig. 3). At the same time, the maximum yield of sorbitol (63 %) also is observed over 1%Ru/Cs-SiW sample (Fig. 3). Such a coincidence cannot be just an accident. Another important point to note is that the catalytic efficiency (TON based on Ru loading) decreases with increasing density of acid sites (Fig. S8, SI). This can indicate decreasing of LAS_{HPA} contribution to the cellulose hydrolysis process.

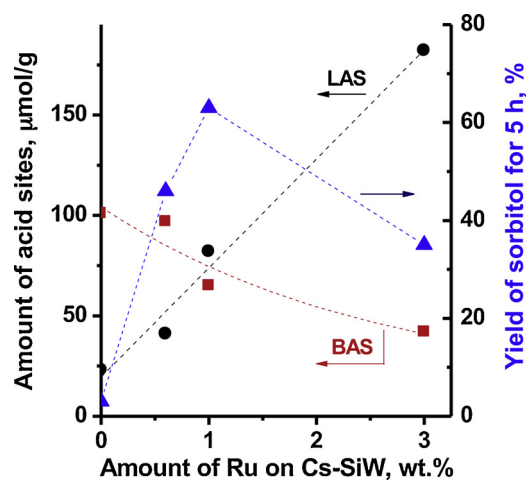


Fig. 3. Dependence of the yield of sorbitol and number of acid sites on the Ru content in Ru/Cs-SiW. (Experimental conditions: 10 g L⁻¹ of cellulose, 10 g L⁻¹ of catalyst, 5 MPa of H₂, 453 K).

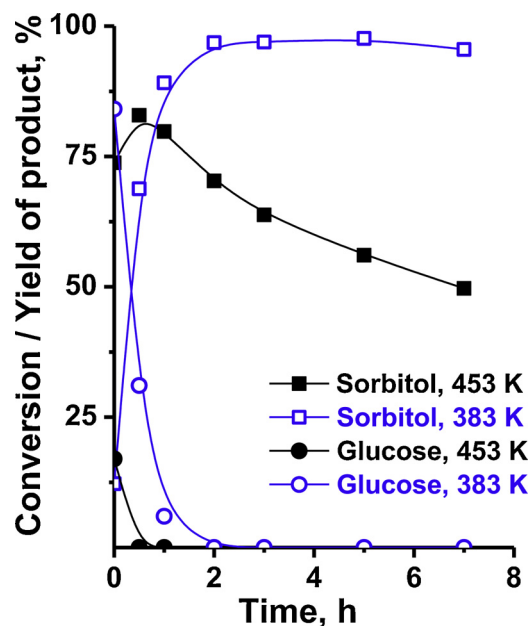


Fig. 4. Kinetic curves of sorbitol accumulation and glucose consumption in hydrolysis-hydrogenation over 1%Ru/Cs-SiW at 383 and 453 K. (Experimental conditions: 10 g L^{-1} of a substrate (cellobiose or glucose), 10 g L^{-1} of catalyst, 5 MPa of H_2).

On the one hand, increasing of the Ru content rises the amount of LAS_{Ru} . They are suggested to be the sites for the adsorption of intermediates (glucose) on the surface of catalyst, its quick hydrogenation. Therefore, the maximal yield of the sorbitol can be archived in the presence of a catalyst with optimal amount of LAS_{Ru} and LAS_{HPA} because the decreasing amount of LAS_{HPA} reduces hydrolysis rate while increasing amount of LAS_{Ru} leads to the strong adsorption of intermediates and in unfavorable spatial orientation for the following transformations.

3.5. Reaction kinetics and pathways over Ru/Cs-HPA

In order to study the cellulose hydrolysis-hydrogenation pathways the transformations of cellobiose and glucose as substrates were studied under conditions identical to the transformation of cellulose. Experiments were conducted at 453 K. Cellobiose was chosen as the simplest saccharide (diccaharide) containing the glycoside bond. From the data obtained, the conversion of glucose to sorbitol was 83 % at the experimental 'zero' point (Fig. 4). The conversion of cellobiose was 90 % under identical conditions (Fig. 5). The observed high conversions may indicate rather high rates of hydrolysis and hydrogenation. Interestingly, the maximal yield of sorbitol (hydrogenation of glucose at 453 K) was 83 % in half an hour of the reaction (74 % at the 'zero' point) (Figs. 4 and 5). After the maximal yield was reached, the concentration of sorbitol decreased to reach ca. 50 % in 7 h. This is an evidence of sorbitol instability at high temperature. At the same time, the overall process is limited by cellulose depolymerization in water, and the rate of this step drops down to almost zero upon even slight temperature reduction; hence, high temperature is necessary for the process. The maximal yield of sorbitol (83 %) observed in the experimental studies of glucose and cellobiose transformations is, again, an evidence of unattainability of 100 % yield of the target product because of its destruction, even though the glucose reduction is a highly selective process. Therefore, glucose hydrogenation was studied over 1%Ru/Cs-SiW at 383 K (Fig. 4). At this low temperature the yield of sorbitol produced from glucose was very high (98 % in 5 h) to indicate very high selectivity of the transformation glucose \rightarrow sorbitol.

The hydrolysis-hydrogenation of cellulose over 1%Ru/Cs-SiW was

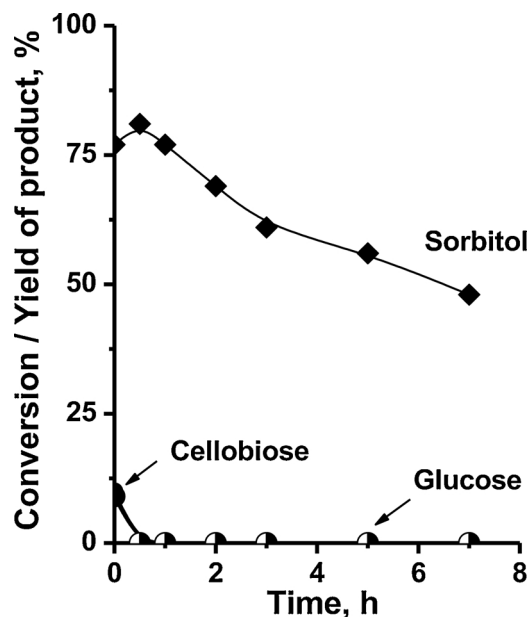


Fig. 5. Kinetic curves of sorbitol accumulation and cellobiose consumption in hydrolysis-hydrogenation over 1%Ru/Cs-SiW at 453 K. (Experimental conditions: 10 g L^{-1} of a substrate (cellobiose or glucose), 10 g L^{-1} of catalyst, 5 MPa of H_2).

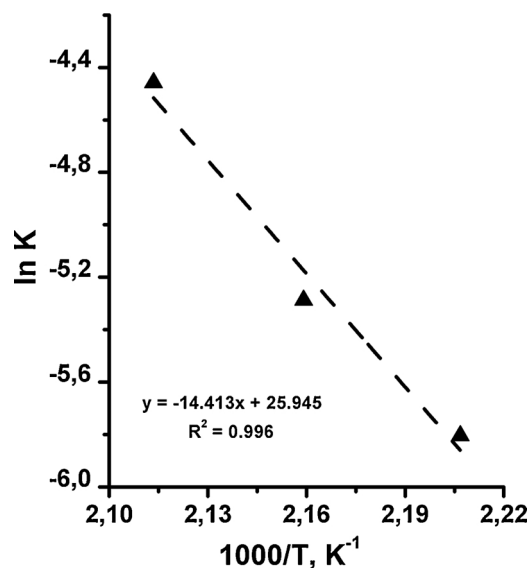
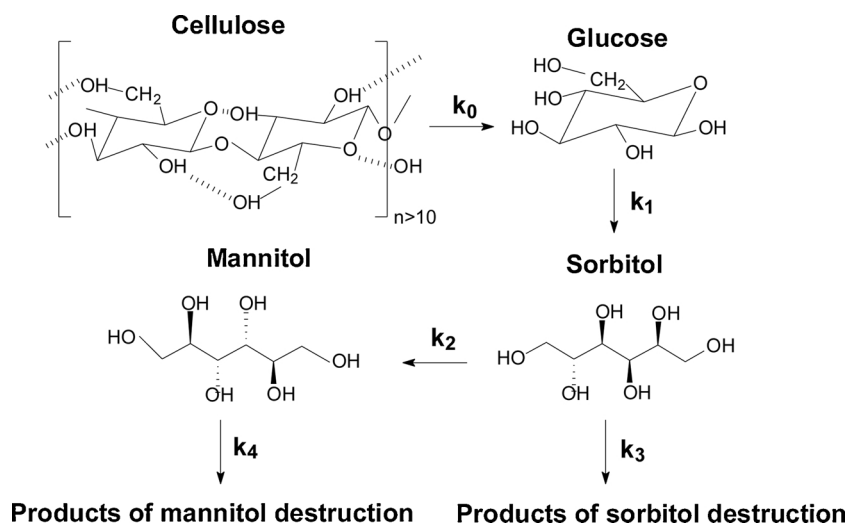


Fig. 6. Arrhenius temperature dependence of initial rate of cellulose hydrolysis-hydrogenation over 1%Ru/Cs-SiW (Experimental conditions: 10 g L^{-1} of cellulose, 10 g L^{-1} of catalyst, 5 MPa of H_2).

studied and the activation energy of the process determined. The activation energy E_a was determined in the process of hydrolysis-hydrogenation of cellulose at 453, 463 and 473 K; $E_a = 120 \pm 5 \text{ kJ mol}^{-1}$ (Fig. 6). This value is much lower as compared to the activation energy found for the processes of cellulose hydrolysis in the solution of sulfuric acid used as a catalyst ($170 - 180 \text{ kJ mol}^{-1}$) [50,51], but close to the activation energy over solid catalysts (sulfonated chloromethyl polystyrene resin, 83 kJ mol^{-1} [52], and sulfonated carbon materials, 110 kJ mol^{-1}) [53,54].

3.6. Modulation of reaction kinetics

The following kinetic model of hydrolysis-hydrogenation of cellulose was suggested in this work (Scheme 2) based on experimental and



Scheme 2. The main steps for modeling of the hydrolysis-hydrogenation of cellulose.

literature data [10,24]. The model includes: (1) cellulose conversion to glucose; (2) reduction of glucose to sorbitol; (3) isomerization of sorbitol to mannitol; (4) side reactions of the product decomposition in the reaction medium at high temperature. Several math models were discussed earlier to describe cellulose hydrolysis-hydrogenation to sorbitol [55,56]. Liu and Liu used a nine-stage model implying the production of ethylene glycol and propylene glycol as the main products of cellulose transformation. It should be emphasized here that glycols were not detected in this work as well as the degradation of sorbitol and mannitol to biochar was out of consideration in the model proposed [55]. Furthermore, the hydrogenation step usually proceeds by the Langmuir–Hinshelwood or the Eley–Rideal mechanism but both can be treated as a pseudo-first-order reaction because of the low concentration of glucose ($< 0.1 \text{ g L}^{-1}$) and excess H_2 .

The second model was suggested by Komanoya et al. [56]. In this model, both amorphous and crystal cellulose can be transformed to the desired products. In our model (Scheme 2) we assume that it is amorphous cellulose that undergoes transformations, while crystal part of the polysaccharide is not reactive [57]. Moreover, the simultaneous formation of hexitols (sorbitol + mannitol) from cellulose was assumed. Although the model in Ref [56] takes into consideration the degradation of hexitols to biochar, we assume (Scheme 2) that the selectivity of sorbitol production from glucose is 100 % (Fig. 4). Hence, mannitol is a side-product of the sorbitol transformation.

The experimental data obtained at 453 K were used for the calculation of the rate constants (Table 3). The constant k_0 was estimated using the experimental data of cellulose conversion (35 % in 1 h) controlled by TOC analysis. The developed kinetic model describes well the experimental data on the hydrolysis-hydrogenation of cellulose (Fig. 7). The modeling was based on the assumption of the observed first order of all the reactions and high rates of adsorption and desorption of the reactants on the catalyst surface. In terms of the model, cellulose is hydrolyzed on the acid sites to glucose to be reduced to sorbitol on the reducing Ru sites of the catalyst. A system of kinetic

Table 3

Rate constants based on the experimental kinetic curves of the hydrolysis/hydrogenation of cellulose catalysed by 1%Ru/Cs-SiW.

Constant	Reaction	Rate constant (min^{-1})
k_0	Cellulose hydrolysis	$7.3 \cdot 10^{-3}$
k_1	Glucose hydrogenation to sorbitol	$5.5 \cdot 10^{-2}$
k_2	Isomerisation of sorbitol to mannitol	$5 \cdot 10^{-4}$
k_3	Sorbitol decomposition	$1.3 \cdot 10^{-3}$
k_4	Mannitol decomposition	$2.5 \cdot 10^{-3}$

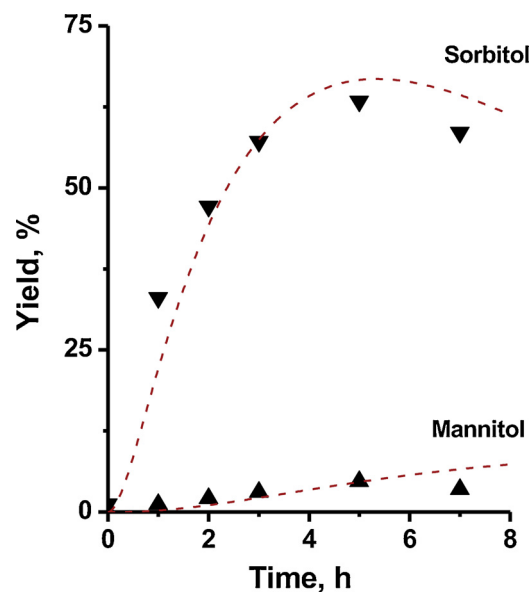


Fig. 7. Experimental (symbol) and theoretical (dash) data for hydrolysis-hydrogenation of mechanically activated cellulose over 1% Ru/Cs-SiW. (Experimental conditions: 10 g L^{-1} of cellulose, 10 g L^{-1} of catalyst, 5 MPa of H_2 , 453 K).

differential Eq.s (I)–(IV) was compiled and resolved using the Mathcad 15.0 program package:

$$\frac{dC_{\text{Cell}}}{dt} = -k_0 \cdot C_{\text{Cell}} \quad (\text{I})$$

$$\frac{dC_{\text{Glu}}}{dt} = k_0 \cdot C_{\text{Cell}} - k_1 \cdot C_{\text{Glu}} \quad (\text{II})$$

$$\frac{dC_{\text{Sorb}}}{dt} = k_1 \cdot C_{\text{Glu}} - k_2 \cdot C_{\text{Sorb}} - k_3 \cdot C_{\text{Sorb}} \quad (\text{III})$$

$$\frac{dC_{\text{Mann}}}{dt} = k_2 \cdot C_{\text{Sorb}} - k_4 \cdot C_{\text{Sorb}} \quad (\text{IV})$$

where Cell is cellulose, Glu is glucose, Sorb is sorbitol, Mann is mannitol.

3.7. Catalytic potential and stability of Ru/Cs-HPA systems

The most active sample 1%Ru/Cs-SiW was studied for three

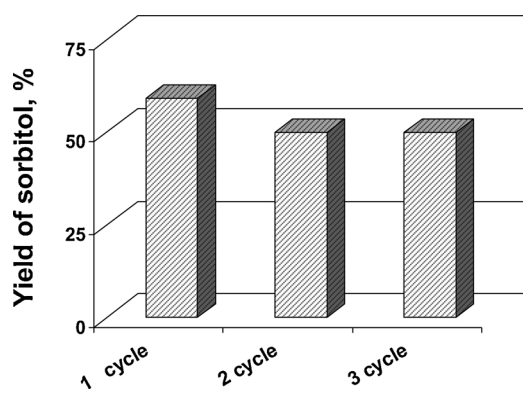


Fig. 8. The yield of sorbitol achieved in three runs over 1%Ru/Cs-SiW catalyst. (Experimental conditions: 10 g L⁻¹ of catalyst, 10 g L⁻¹ of cellulose, 5 MPa of H₂, 453 K).

successive cycles of cellulose hydrolysis-hydrogenation. The Ru/Cs-HPA catalyst demonstrated quite stable catalytic activity. The yield of sorbitol decreased from 59 % (first run) to 50 % (second and third runs) (Fig. 8). The ICP-AES data showed no change in the metal content during the reaction. We suppose that the catalyst activity decreased due to an increase of Ru nanoparticles in average size: the diameter of Ru rose up from 1.1 to 1.5 nm after the first cycle of the reaction while interatomic Ru-Ru distance remained equal to 2.1 Å in both not tested and tested samples (Fig. 1C and 1F). Other reason of decreasing activity can be related with partial leaching of HPA from the samples that is following from the change of the solution pH after reaction from 3.8 to 3.4. Figure S5 (SI) shows XRD patterns of the 1%Ru/Cs-SiW after the first reaction cycle. One can see from these data, the intensities of the peaks in the regions of 32–40 and 15–27 °(2 theta) attributed to the amorphous cellulose strongly decreased due to the reaction. At the same time, the crystallinity of the remain cellulose increased from 36 to 73 %.

We compared the catalytic properties of Ru/Cs-HPA catalytic systems with the properties of the systems reported in the literature (Table 4). One can see that the catalysts suggested earlier are active under more severe conditions. Since the conditions for the sample testing are different, we compared the effectiveness of catalysts based on TOF calculated by formula:

$$TOF_{Ru} = \frac{\sum m_{Sorbitol+Mannitol}}{m_{Ru} \times \tau}$$

where, $\sum m_{Sorbitol+mannitol}$ is total amount of sorbitol and mannitol (g), m_{Ru} is the Ru loading in a catalyst (g), τ is the reaction time (h).

In general, the Ru/Cs-PW and Ru/Cs-SiW systems under study are

Table 4

Comparison of catalytic properties of Ru-containing systems based on HPA in hydrolysis-hydrogenation of cellulose.

N	Catalyst	Experimental conditions				Catalytic test				TOF (g/(h·g _{Ru}))	Ref
		T (K)	P (MPa)	Time (h)	Cell/Cat (g/g)	Sorbitol		Mannitol			
						S (%)	Y (%)	S (%)	Y (%)		
1	1%Ru/ Cs _{2.1} H _{0.9} PW ₁₂ O ₄₀	453	5	3	0.45/0.45	97	38	3	1	13.7	This work
2	1%Ru/Cs ₃ HSiW ₁₂ O ₄₀	453	5	3	0.45/0.45	95	58	5	3	20.3	
3	3%Ru/C + Cs ₃ HSiW ₁₂ O ₄₀	453	5	3	0.45/(0.45 + 0.45)	86	13	14	2	1.7	
4	3%Ru/C	453	5	3	0.45/0.45	9	1	38	4	0.017	
5	1%Ru/Cs ₃ PW ₁₂ O ₄₀	433	2	24	0.10/0.10		43		2.1	0.6	[25]
6	5 wt% Ru/C + Cs _{2.5} H _{0.5} PW ₁₂ O ₄₀	463	5	8	1/(0.25 + 0.5)	56 [a]				5.6	[19]
7	5 wt% Ru/C + Cs _{3.5} H _{0.5} SiW ₁₂ O ₄₀	463	5	13	1/(0.25 + 0.5)	59 [a]				3.6	[19]
8	3.2%Ru/16.7 %H ₃ PW ₁₂ O ₄₀ /MIL-100(Cr)	463	2	10	0.050/0.03		57.9		6.6	3.3	[46]
9	0.4 wt%Ru/ H ₃ PW ₁₂ O ₄₀ /AC	478	5	5	0.75/0.3		17		n.d.	18.9	[58]
10	0.4 wt%Ru/ H ₄ SiW ₁₂ O ₄₀ /AC	478	5	5	0.75/0.3		12		n.d.	13.3	[58]

[a] Total yield of sorbitol + mannitol.

much more active than the systems described elsewhere (Table 4). Comparing the activity of mechanical mixtures Ru/C + Cs-HPA shows that the mechanical mixture Ru/C + Cs_{2.5}H_{0.5}PW₁₂O₄₀ (1:2 wt./wt.) [19,25] is more active compared to the mixture Ru/C + Cs-SiW (Table 4, runs 3, 6, 7) that is thought to result from the higher acidity of the reaction mixture due to the higher Cs-HPA content. The low activity of the 1%Ru/Cs₃PW₁₂O₄₀ system demonstrated by Liu et al. [25] as compared with the system under study may be caused by milder reaction conditions (low temperature and pressure) (Table 4, runs 1, 5).

Comparative studies of catalytic properties of Ru/Cs-HPA systems and the mechanical mixture of Ru/C + Cs-SiW (1:1 wt./wt.) revealed significant advantage of the bifunctional Ru/Cs-HPA systems (Table 4, runs 1-3). First, the application of Ru/Cs-HPA systems allows the selectivity to sorbitol to be improved by 46 % and the yield of mannitol as the side product to be decreased from 10 % to 4–7 %. Especially noticeable is the fact that the yield of sorbitol over Ru/Cs-HPA systems is much higher of that over the Ru/C and mechanical mixture of Ru/C + Cs-SiW (1:1 wt./wt.) (Table 4, runs 1–4). A significant disadvantage of the mechanical mixture is decreasing the total yield because of the biochar formation (Table 2, lines 13, 14). Acid sites located on CsHPA and reducing sites located on Ru/C are divided from each other in two component system. Therefore, the intermediates of hydrolysis should be transferred from CsHPA acid catalyst to Ru/C reducing catalytic system. The transfer needs much longer time compared to the bifunctional catalyst Ru/CsHPA, that favors the formation of biochar. At the same time, the high yield of sorbitol may be accounted for by synergetic effect caused by the spatial proximity of the acidic and reducing sites on the Ru/Cs-HPA surface where the reactions of hydrolysis and hydrogenation proceed, respectively. Their proximity allows the diffusion limitations and the necessity of intermediate transferring from acid sites for hydrolysis to metal sites for reduction to be lowered.

4. Conclusions

Bifunctional catalysts based on cesium salts of heteropolyacids (HPA) (Cs_{2.1}H_{0.9}PW₁₂O₄₀ and Cs₃HSiW₁₂O₄₀) and Ru nanoparticles were prepared by impregnation of polyoxometalates by Ru(NO)(NO₃)₃ followed by reduction of the precursor to produce Ru nanoparticles. The Ru/Cs-PW and Ru/Cs-SiW catalysts were characterized by elemental analysis, X-ray powder diffraction (XRD), N₂-adsorption/desorption analysis, transmission electron microscopy (TEM), Fourier-transform infrared spectroscopy (FT-IR), Diffuse Reflectance Ultraviolet-visible spectroscopy (DR UV-vis). TEM studies confirmed that highly dispersed Ru particles (0.9–1.4 nm in size) were stabilized on the Cs-HPA surface.

Catalytic properties of Ru/Cs-PW and Ru/Cs-SiW were studied in one-pot hydrolysis-hydrogenation of mechanically activated microcrystalline cellulose to sorbitol under hydrothermal conditions at 453 K and hydrogen pressure 5 MPa. The yields of the main product were in the range of 36–59 % and the selectivity of sorbitol formation was 94–96 % over of Ru/Cs-HPA. The highest yield of sorbitol (59 %) was obtained over 1%Ru/Cs-SiW catalyst in 7 h of the reaction.

A correlation between the number of Brønsted acid sites and catalytic activity was established. The catalyst activity increased with rising BAS numbers to confirm that the process was limited by polysaccharide hydrolysis. The Ru content in the catalyst, nanoparticle size and ru oxidative state affected both the hydrolysis and hydrogenation steps.

The activation energy of hydrolysis-hydrogenation of cellulose over the most active catalyst 1%Ru/Cs-SiW was calculated to equal to $120 \pm 5 \text{ kJ}\cdot\text{mol}^{-1}$. A kinetic scheme of hydrolysis-hydrogenation over 1%Ru/Cs-SiW catalysts was suggested and rate constants were calculated. The suggested scheme described quantitatively the experimental results. Bifunctional catalysts were demonstrated to be much more active and selective than the Ru/C catalyst and mechanical mixture of Ru/C + Cs-HPA.

CRedit authorship contribution statement

Nikolay V. Gromov: Investigation, Formal analysis, Writing - original draft. **Tatiana B. Medvedeva:** Data curation, Visualization. **Oxana P. Taran:** Writing - review & editing, Project administration. **Maria N. Timofeeva:** Writing - review & editing. **Oliver Said-Aizpuru:** Investigation. **Valentina N. Panchenko:** Methodology, Resources. **Evgeniy Yu. Gerasimov:** Methodology, Resources. **Ivan V. Kozhevnikov:** Supervision. **Valentin N. Parmon:** Conceptualization, Funding acquisition.

Declaration of Competing Interest

The authors declare that they have no known competing financial interests or personal relationships that could have appeared to influence the work reported in this paper.

Acknowledgements

This work was supported by the Russian Foundation for Basic Research (Project 17-43-540664).

Appendix A. Supplementary data

Supplementary material related to this article can be found, in the online version, at doi:<https://doi.org/10.1016/j.apcata.2020.117489>.

References

- [1] P. Bhaumik, P.L. Dhepe, Catal. Rev. 58 (2016) 36–112, <https://doi.org/10.1080/01614940.2015.1099894>.
- [2] R.-J. van Putten, J.C. van der Waal, E. de Jong, C.B. Rasrendra, H.J. Heeres, J.G. de Vries, Chem. Rev. 113 (2013) 1499–1597, <https://doi.org/10.1021/cr300182k>.
- [3] M. Besson, P. Gallezot, C. Pinel, Chem. Rev. 114 (2014) 1827–1870, <https://doi.org/10.1021/cr4002269>.
- [4] A. Bruggink, R. Schoevaart, T. Kieboom, Org. Process Res. Dev. 7 (2003) 622–640, <https://doi.org/10.1021/op0340311>.
- [5] P. Gallezot, A. Kiennemann, G. Ertl, H. Knözinger, F. Schüth, J. Weitkamp (Eds.), Handbook of Heterogeneous Catalysis, Wiley-VCH Verlag GmbH & Co. KGaA, 2008.
- [6] D.Y. Murzin, I.L. Simakova, J. Reedijk, K. Poepplmeier (Eds.), Comprehensive Inorganic Chemistry II (Second Edition), Elsevier, Amsterdam, 2013, pp. 559–586.
- [7] E.M. Sulman, V.Y. Doluda, V.G. Matveeva, M.E. Grigorev, M.G. Sulman, A.V. Bykov, Chem. Eng. Res. Des. 52 (2016) 673–678, <https://doi.org/10.3303/CET1652113>.
- [8] H. Li, W. Wang, J. Fa Deng, J. Catal. 191 (2000) 257–260, <https://doi.org/10.1006/jcat.1999.2792>.
- [9] A.A. Balandin, N.A. Vasyunina, S.V. Chepigo, G.S. Barysheva, Dokl. Akad. Nauk SSSR 128 (1959) 941.
- [10] W. Deng, Y. Wang, Q. Zhang, Y. Wang, Catal. Surveys Asia 16 (2012) 91–105, <https://doi.org/10.1007/s10563-012-9136-1>.

- [11] H. Li, Z. Fang, R.L. Smith, S. Yang, Prog. Energy Comb. Sci. 55 (2016) 98–194, <https://doi.org/10.1016/j.pecs.2016.04.004>.
- [12] J. Geboers, S. Van de Vyver, K. Carpentier, K. de Blochouse, P. Jacobs, B. Sels, Chem. Comm. 46 (2010) 3577–3579, <https://doi.org/10.1039/C001096K>.
- [13] Y. Li, Y. Liao, X. Cao, T. Wang, L. Ma, J. Long, Q. Liu, Y. Xua, Biomass Bioenergy 74 (2015) 148–161, <https://doi.org/10.1016/j.biombioe.2014.12.025>.
- [14] X. Zhao, J. Xu, A. Wang, T. Zhang, Chin. J. Catal. 36 (9) (2015) 1419–1427, [https://doi.org/10.1016/S1872-2067\(15\)60942-1](https://doi.org/10.1016/S1872-2067(15)60942-1).
- [15] H. Kobayashi, Y. Ito, T. Komanoya, Y. Hosaka, P.L. Dhepe, K. Kasai, K. Hara, A. Fukuoka, Green Chem. 13 (2011) 326–333, <https://doi.org/10.1039/C0GC00666A>.
- [16] R. Palkovits, K. Tajvidi, J. Procelewska, R. Rinaldi, A. Ruppert, Green Chem. 12 (2010) 972–978, <https://doi.org/10.1039/C000075B>.
- [17] H. Li, Q. Zhang, A. Riisager, S. Yang, Current Nanosci. 11 (2015) 1–14, <https://doi.org/10.2174/1573413710666141010215429>.
- [18] W. Deng, Q. Zhang, Y. Wang, Dalton Trans. 41 (2012) 9817–9831, <https://doi.org/10.1039/C2DT30637A>.
- [19] J. Geboers, S. Van de Vyver, K. Carpentier, P. Jacobs, B. Sels, Green Chem. 13 (2011) 2167–2174, <https://doi.org/10.1039/C1GC15350A>.
- [20] G. Liang, C. Wu, L. He, J. Ming, H. Cheng, L. Zhuo, F. Zhao, Green Chem. 13 (2011) 839–842, <https://doi.org/10.1039/c1gc15098g>.
- [21] T. Ennaert, S. Feys, D. Hendrikx, P.A. Jacobs, B.F. Sels, Green Chem. 18 (2016) 5295–5304, <https://doi.org/10.1039/C6GC01439A>.
- [22] D.Y. Murzin, E.V. Murzina, A. Tokarev, N.D. Shcherban, J. Wärnå, T. Salmi, Catal. Today 257 (2015) 169–176, <https://doi.org/10.1016/j.cattod.2014.07.019>.
- [23] D. Reyes-Luyanda, J. Flores-Cruz, P.J. Morales-Pérez, L.G. Encarnación-Gómez, F. Shi, P.M. Voyles, N. Cardona-Martínez, Top. Catal. 55 (2012) 148–161, <https://doi.org/10.1007/s11244-012-9791-5>.
- [24] A. Fukuoka, P.L. Dhepe, Angew. Chem. 118 (2006) 5285–5287, <https://doi.org/10.1002/ange.200601921>.
- [25] M. Liu, W. Deng, Q. Zhang, Y. Wang, Y. Wang, Chem. Comm. 47 (2011) 9717–9719, <https://doi.org/10.1039/C1CC12506K>.
- [26] J. Tian, C. Fang, M. Cheng, X. Wang, Chem. Eng. Technol. 34 (2011) 482–486, <https://doi.org/10.1002/ceat.201000409>.
- [27] Y. Ogasawara, S. Itagaki, K. Yamaguchi, N. Mizuno, ChemSusChem 4 (2011) 519–525, <https://doi.org/10.1002/cssc.201100025>.
- [28] K.-i. Shimizu, H. Furukawa, N. Kobayashi, Y. Itaya, A. Satsuma, Green Chem. 11 (2009) 1627–1632, <https://doi.org/10.1039/B913737H>.
- [29] C.R. Henry, Appl. Surface Sci. 164 (2000) 252–259, [https://doi.org/10.1016/S0169-4332\(00\)00344-5](https://doi.org/10.1016/S0169-4332(00)00344-5).
- [30] R. Schlögl, S.B. Abd Hamid, Angew. Chem. Int. Ed. 43 (2004) 1628–1637, <https://doi.org/10.1002/anie.200301684>.
- [31] R.A. Van Santen, Acc. Chem. Res. 42 (2009) 57–66, <https://doi.org/10.1021/ar800022m>.
- [32] I.L. Simakova, Y.S. Demidova, J. Glasel, E.V. Murzina, T. Schubert, I.P. Prosvirin, B.J.M. Etzold, D.Y. Murzin, Catal. Sci. Technol. 6 (2016) 8490–8504, <https://doi.org/10.1039/C6CY02086K>.
- [33] H. Kobayashi, H. Matsuhashi, T. Komanoya, K. Hara, A. Fukuoka, Chem. Comm. 47 (2011) 2366–2368, <https://doi.org/10.1039/C0CC04311G>.
- [34] S. Park, J.O. Baker, M.E. Himmel, P.A. Parilla, D.K. Johnson, Biotechnol. Biofuels 3 (2010) 10, <https://doi.org/10.1186/1754-6834-3-10>.
- [35] A.K. Ghosh, J.B. Moffat, J. Catal. 101 (1986) 238–245, [https://doi.org/10.1016/0021-9517\(86\)90249-6](https://doi.org/10.1016/0021-9517(86)90249-6).
- [36] D.P. Minh, G. Aubert, P. Gallezot, M. Besson, Appl. Catal. B: Env. 73 (2007) 236–246, <https://doi.org/10.1016/j.apcatb.2006.12.014>.
- [37] A.B. Ayusheev, O.P. Taran, I.A. Seryak, O.Y. Podyacheva, C. Descorme, M. Besson, L.S. Kibis, A.I. Boronin, A.I. Romanenko, Z.R. Ismagilov, V. Parmon, Appl. Catal. B 146 (2014) 177–185, <https://doi.org/10.1016/j.apcatb.2013.03.017>.
- [38] S.V. Tsybulya, S.V. Cherepanova, L.P. Soloviyova, J. Struct. Chem. 37 (1996) 332–334, <https://doi.org/10.1007/BF02591064>.
- [39] A.A. Davydov, Molecular Spectroscopy of Oxide Catalyst Surfaces, John Wiley & Sons, Chichester, 2003.
- [40] N.V. Gromov, O.P. Taran, I.V. Delidovich, A.V. Pestunov, Yu.A. Rodikova, D.A. Yatsenko, E.G. Zhizhina, V.N. Parmon, Catal. Today 278 (2016) 74–81, <https://doi.org/10.1016/j.cattod.2016.03.030>.
- [41] N.V. Gromov, T.B. Medvedeva, O.P. Taran, A.V. Bukhtiyarov, C. Aymonier, I.P. Prosvirin, V.N. Parmon, Topics Catal. 61 (2018) 1912–1927, <https://doi.org/10.1007/s11244-018-1049-4>.
- [42] N.V. Gromov, O.P. Taran, K.N. Sorokina, T.I. Mishchenko, S. Uthandi, V.N. Parmon, Catal. Use Indium 8 (2016) 176–186, <https://doi.org/10.1134/S2070050416020057>.
- [43] I.V. Kozhevnikov, Catalysts for Fine Chemical Synthesis, Catalysis by Polyoxometalates Volume 2 Wiley-VCH, Liverpool, 2002.
- [44] A.M. Raspolli Galletti, C. Antonetti, I. Longo, G. Capannelli, A.M. Venezia, Appl. Catal. A 350 (2008) 46–52, <https://doi.org/10.1016/j.apcata.2008.07.044>.
- [45] J. Chen, S. Wang, J. Huang, L. Chen, L. Ma, X. Huang, ChemSusChem 6 (8) (2013) 1545–1555, <https://doi.org/10.1002/cssc.201200914>.
- [46] X. Xie, J. Han, H. Wang, X. Zhu, X. Liu, Y. Niu, Z. Song, Q. Ge, Catal. Today 233 (2014) 70–76, <https://doi.org/10.1016/j.cattod.2013.09.061>.
- [47] M.-Y. Zheng, A.-Q. Wang, N. Ji, J.-F. Pang, X.-D. Wang, T. Zhang, ChemSusChem 3 (2010) 63–66, <https://doi.org/10.1002/cssc.200900197>.
- [48] N. Ji, T. Zhang, M. Zheng, A. Wang, H. Wang, X. Wang, J.G. Chen, Angew. Chem. Int. Ed. 47 (2008) 8510–8513, <https://doi.org/10.1002/anie.200803233>.
- [49] A. Wang, T. Zhang, Acc. Chem. Res. 46 (2013) 1377–1386, <https://doi.org/10.1021/ar3002156>.
- [50] B. Girisuta, L.P.B.M. Janssen, H.J. Heeres, Green Chem. 8 (2006) 701–709, <https://doi.org/10.1039/B5GC00000A>.

- doi.org/10.1039/B518176C.
- [51] L.V.A. Gurgel, K. Marabezi, L.A. Ramos, A.Ad.S. Curvelo, *Ind. Crops Prod.* 36 (2012) 560–571, <https://doi.org/10.1016/j.indcrop.2011.11.009>.
- [52] L. Shuai, X. Pan, *Energy Env. Sci.* 5 (2012) 6889–6894, <https://doi.org/10.1039/C2EE03373A>.
- [53] S. Suganuma, K. Nakajima, M. Kitano, D. Yamaguchi, H. Kato, S. Hayashi, M. Hara, *J. Am. Chem. Soc.* 130 (2008) 12787–12793, <https://doi.org/10.1021/ja803983h>.
- [54] D. Yamaguchi, M. Kitano, S. Suganuma, K. Nakajima, H. Kato, M. Hara, *J. Phys. Chem. C* 113 (2009) 3181–3188, <https://doi.org/10.1021/jp808676d>.
- [55] Y. Liu, H. Liu, *Catal. Today* 269 (2016) 74–81, <https://doi.org/10.1016/j.cattod.2015.09.056>.
- [56] T. Komanoya, H. Kobayashi, K. Hara, W.-J. Chun, A. Fukuofa, *ChemCatChem* 6 (1) (2014) 230–236, <https://doi.org/10.1002/cctc.201300731>.
- [57] N.V. Gromov, *Catalytic Methods of Cellulose Transformation in Pure Water into Valuable Chemical Substances*, PhD Thesis, supervisors Dr. C. Aymonier, Dr. O. Taran, Boreskov Institute of Catalysis, Novosibirsk, 2016.
- [58] M. Almohalla, I. Rodríguez-Ramos, L.S. Ribeiro, J.J.M. Órfão, M.F.R. Pereira, A. Guerrero-Ruiz, *Catal. Today* 301 (2018) 65–71, <https://doi.org/10.1016/j.cattod.2017.05.023>.